Figure S1

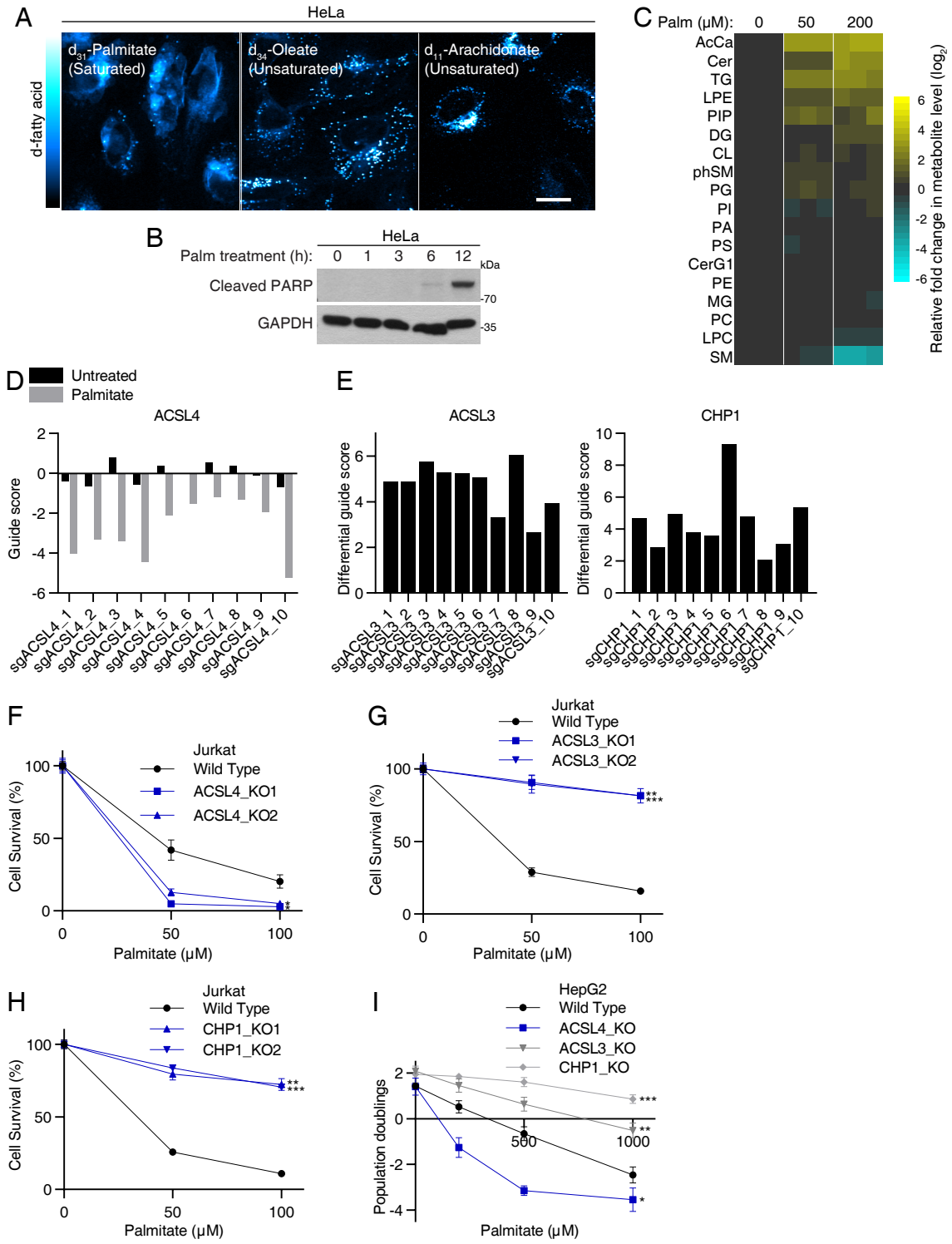
A
HeLa
d-fatty acid
d31-Palmitate (Saturated)
d34-Oleate (Unsaturated)
d11-Arachidonate (Unsaturated)
B
HeLa
Palm treatment (h): 0 1 3 6 12
kDa
Cleaved PARP
GAPDH
-70
-35
C
Palm (μM): 0 50 200
AcCa
Cer
TG
LPE
PIP
DG
CL
phSM
PG
PI
PA
PS
CerG1
PE
MG
PC
LPC
SM
Relative fold change in metabolite level (log2)
D
Untreated
Palmitate
ACSL4
Guide score
sgACSL4_1
sgACSL4_2
sgACSL4_3
sgACSL4_4
sgACSL4_5
sgACSL4_6
sgACSL4_7
sgACSL4_8
sgACSL4_9
sgACSL4_10
E
ACSL3
Differential guide score
sgACSL3_1
sgACSL3_2
sgACSL3_3
sgACSL3_4
sgACSL3_5
sgACSL3_6
sgACSL3_7
sgACSL3_8
sgACSL3_9
sgACSL3_10
CHP1
Differential guide score
sgCHP1_1
sgCHP1_2
sgCHP1_3
sgCHP1_4
sgCHP1_5
sgCHP1_6
sgCHP1_7
sgCHP1_8
sgCHP1_9
sgCHP1_10
F
Jurkat
Wild Type
ACSL4_KO1
ACSL4_KO2
Cell Survival (%)
Palmitate (μM)
G
Jurkat
Wild Type
ACSL3_KO1
ACSL3_KO2
Cell Survival (%)
Palmitate (μM)
H
Jurkat
Wild Type
CHP1_KO1
CHP1_KO2
Cell Survival (%)
Palmitate (μM)
I
HepG2
Wild Type
ACSL4_KO
ACSL3_KO
CHP1_KO
Population doublings
Palmitate (μM)

Figure S2

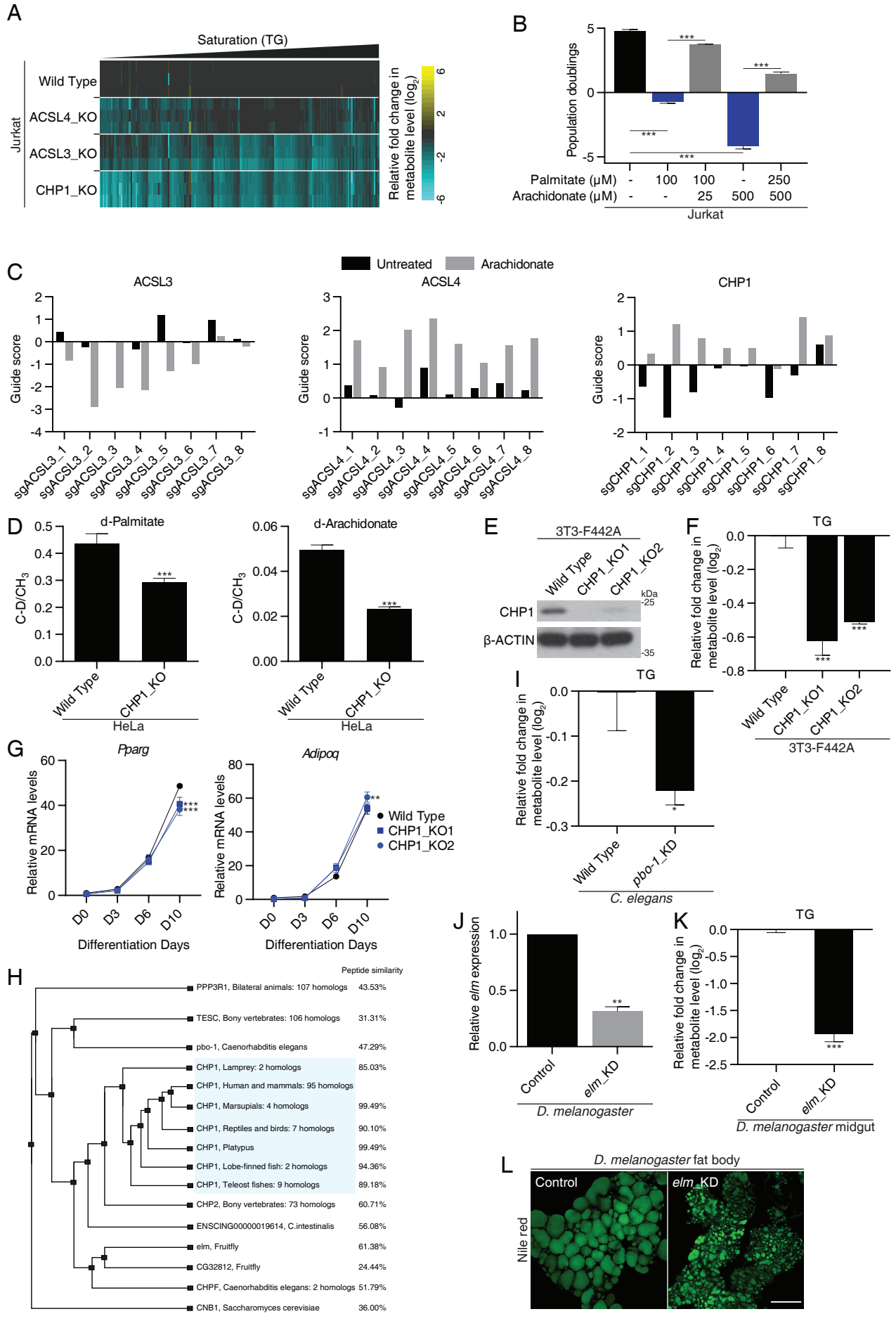
A
Saturation (TG)
Wild Type
ACSL4_KO
ACSL3_KO
CHP1_KO
Jurkat
Relative fold change in metabolite level (log2)
B
Population doublings
Palmitate (μM)
Arachidonate (μM)
Jurkat
C
Untreated
Arachidonate
ACSL3
ACSL4
CHP1
Guide score
D
d-Palmitate
d-Arachidonate
C-D/CH3
Wild Type
CHP1_KO
HeLa
E
3T3-F442A
CHP1
β-ACTIN
kDa
F
TG
Relative fold change in metabolite level (log2)
3T3-F442A
G
Pparg
Adipoq
Relative mRNA levels
Differentiation Days
H
Peptide similarity
PPP3R1, Bilateral animals: 107 homologs 43.53%
TESC, Bony vertebrates: 106 homologs 31.31%
pbo-1, Caenorhabditis elegans 47.29%
CHP1, Lamprey: 2 homologs 85.03%
CHP1, Human and mammals: 95 homologs
CHP1, Marsupials: 4 homologs 99.49%
CHP1, Reptiles and birds: 7 homologs 90.10%
CHP1, Platypus 99.49%
CHP1, Lobe-finned fish: 2 homologs 94.36%
CHP1, Teleost fishes: 9 homologs 89.18%
CHP2, Bony vertebrates: 73 homologs 60.71%
ENSCING00000019614, C.intestinalis 56.08%
elm, Fruitfly 61.38%
CG32812, Fruitfly 24.44%
CHPF, Caenorhabditis elegans: 2 homologs 51.79%
CNB1, Saccharomyces cerevisiae 36.00%
I
TG
C. elegans
J
Relative elm expression
D. melanogaster
K
TG
D. melanogaster midgut
L
D. melanogaster fat body
Control
elm_KD
Nile red

Figure S3

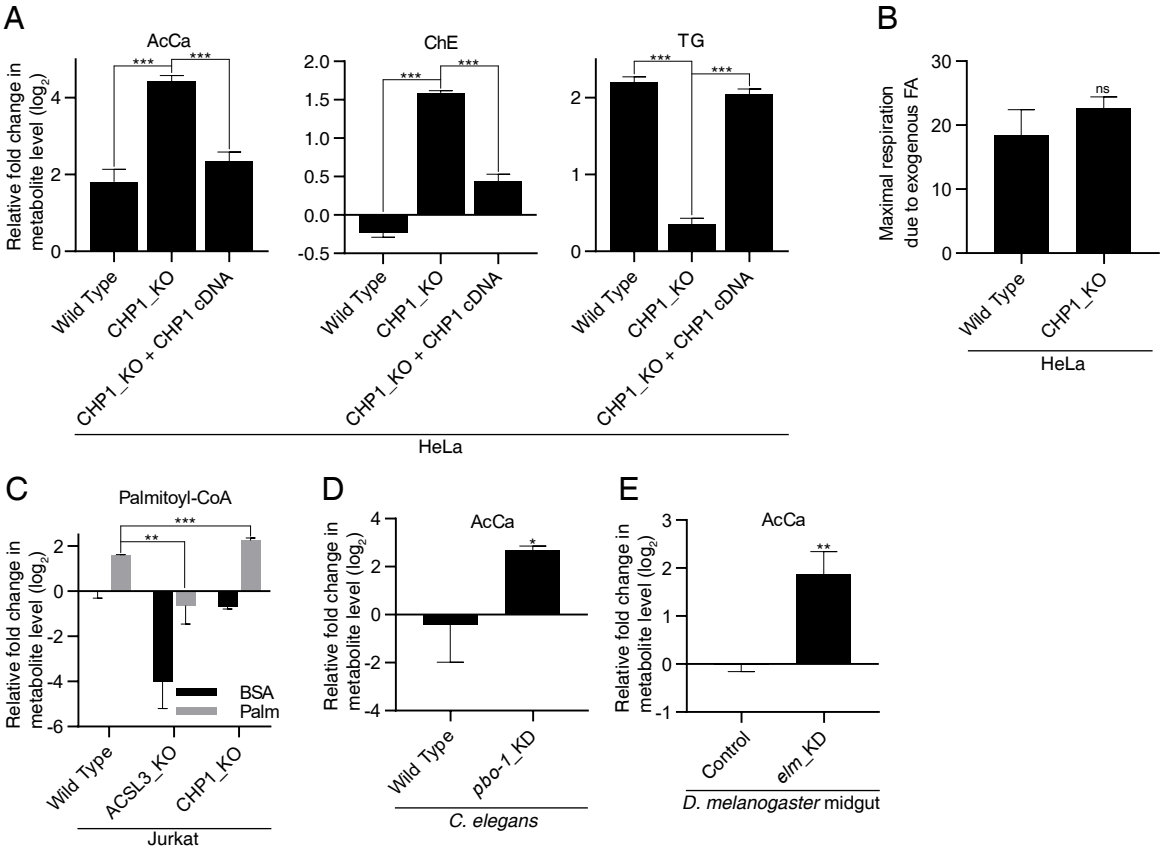
A
AcCa
ChE
TG
Relative fold change in metabolite level (log2)
Wild Type
CHP1_KO
CHP1_KO + CHP1 cDNA
HeLa
B
Maximal respiration due to exogenous FA
ns
Wild Type
CHP1_KO
HeLa
C
Palmitoyl-CoA
BSA
Palm
Wild Type
ACSL3_KO
CHP1_KO
Jurkat
D
AcCa
Wild Type
pbo-1_KD
C. elegans
E
AcCa
Control
elm_KD
D. melanogaster midgut

Figure S4

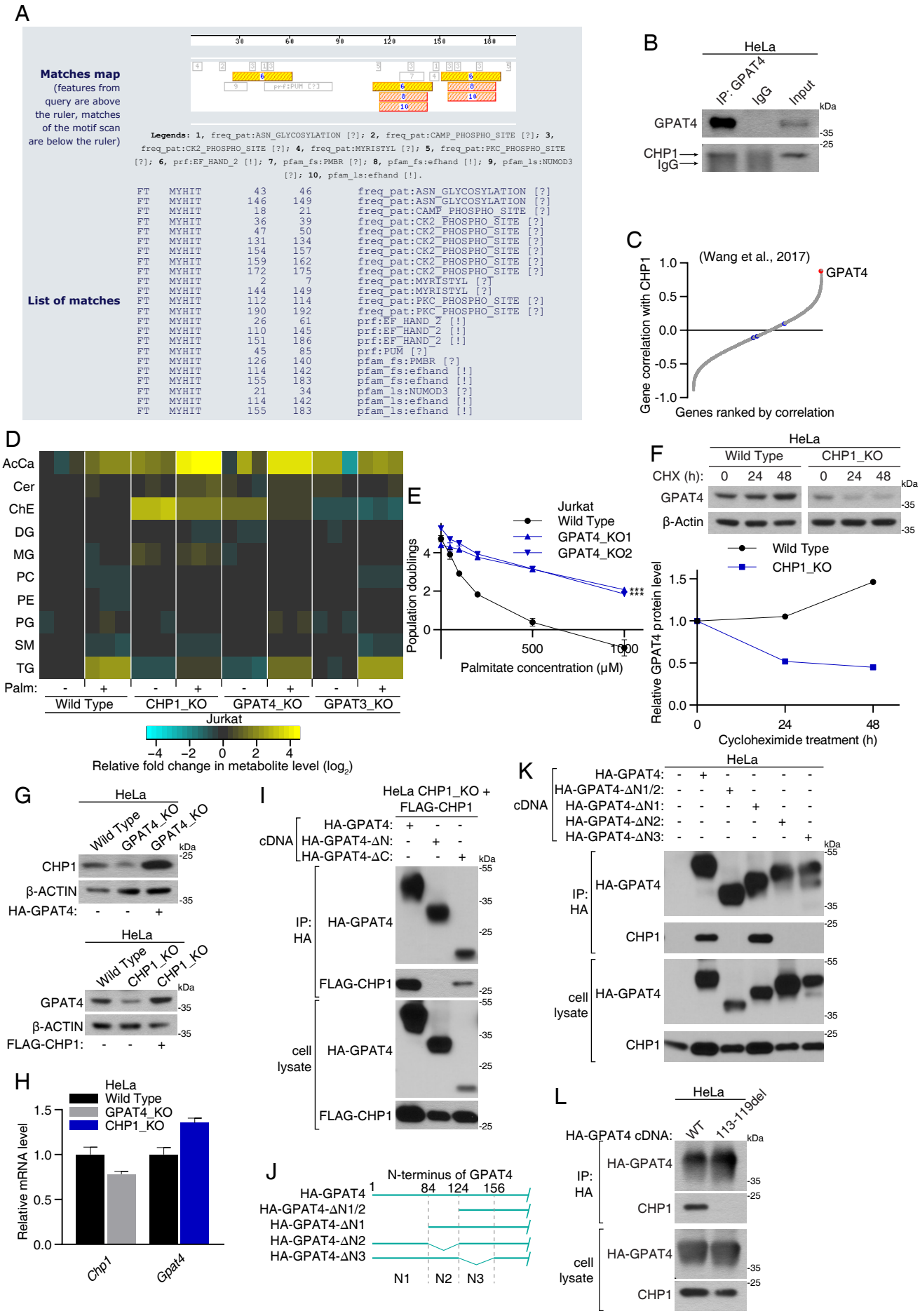
A
Matches map
(features from query are above the ruler, matches of the motif scan are below the ruler)
Legends: 1, freq_pat:ASN_GLYCOSYLATION [?]; 2, freq_pat:CAMP_PHOSPHO_SITE [?]; 3, freq_pat:CK2_PHOSPHO_SITE [?]; 4, freq_pat:MYRISTYL [?]; 5, freq_pat:PKC_PHOSPHO_SITE [?]; 6, prf:EF_HAND_2 [!]; 7, pfam_fs:PMBR [?]; 8, pfam_fs:efhand [!]; 9, pfam_ls:NUMOD3 [?]; 10, pfam_ls:efhand [!].
List of matches
FT MYHIT 43 46 freq_pat:ASN_GLYCOSYLATION [?]
FT MYHIT 146 149 freq_pat:ASN_GLYCOSYLATION [?]
FT MYHIT 18 21 freq_pat:CAMP_PHOSPHO_SITE [?]
FT MYHIT 36 39 freq_pat:CK2_PHOSPHO_SITE [?]
FT MYHIT 47 50 freq_pat:CK2_PHOSPHO_SITE [?]
FT MYHIT 131 134 freq_pat:CK2_PHOSPHO_SITE [?]
FT MYHIT 154 157 freq_pat:CK2_PHOSPHO_SITE [?]
FT MYHIT 159 162 freq_pat:CK2_PHOSPHO_SITE [?]
FT MYHIT 172 175 freq_pat:CK2_PHOSPHO_SITE [?]
FT MYHIT 2 7 freq_pat:MYRISTYL [?]
FT MYHIT 144 149 freq_pat:MYRISTYL [?]
FT MYHIT 112 114 freq_pat:PKC_PHOSPHO_SITE [?]
FT MYHIT 190 192 freq_pat:PKC_PHOSPHO_SITE [?]
FT MYHIT 26 61 prf:EF_HAND_2 [!]
FT MYHIT 110 145 prf:EF_HAND_2 [!]
FT MYHIT 151 186 prf:EF_HAND_2 [!]
FT MYHIT 45 85 prf:PUM [?]
FT MYHIT 126 140 pfam_fs:PMBR [?]
FT MYHIT 114 142 pfam_fs:efhand [!]
FT MYHIT 155 183 pfam_fs:efhand [!]
FT MYHIT 21 34 pfam_ls:NUMOD3 [?]
FT MYHIT 114 142 pfam_ls:efhand [!]
FT MYHIT 155 183 pfam_ls:efhand [!]
B
HeLa
IP: GPAT4
IgG
Input
kDa
GPAT4
CHP1
IgG
-35
-25
C
(Wang et al., 2017)
GPAT4
Gene correlation with CHP1
Genes ranked by correlation
D
AcCa
Cer
ChE
DG
MG
PC
PE
PG
SM
TG
Palm:
Wild Type
CHP1_KO
GPAT4_KO
GPAT3_KO
Jurkat
Relative fold change in metabolite level (log2)
E
Jurkat
Wild Type
GPAT4_KO1
GPAT4_KO2
Population doublings
Palmitate concentration (μM)
F
HeLa
Wild Type
CHP1_KO
CHX (h):
GPAT4
β-Actin
Relative GPAT4 protein level
Cycloheximide treatment (h)
G
HeLa
Wild Type
GPAT4_KO
CHP1
β-ACTIN
HA-GPAT4:
GPAT4
FLAG-CHP1:
H
HeLa
Wild Type
GPAT4_KO
CHP1_KO
Relative mRNA level
Chp1
Gpat4
I
HeLa CHP1_KO + FLAG-CHP1
cDNA
HA-GPAT4:
HA-GPAT4-ΔN:
HA-GPAT4-ΔC:
IP: HA
HA-GPAT4
FLAG-CHP1
cell lysate
J
N-terminus of GPAT4
HA-GPAT4
HA-GPAT4-ΔN1/2
HA-GPAT4-ΔN1
HA-GPAT4-ΔN2
HA-GPAT4-ΔN3
N1
N2
N3
K
HeLa
cDNA
HA-GPAT4:
HA-GPAT4-ΔN1/2:
HA-GPAT4-ΔN1:
HA-GPAT4-ΔN2:
HA-GPAT4-ΔN3:
IP: HA
HA-GPAT4
CHP1
cell lysate
L
HeLa
HA-GPAT4 cDNA:
WT
113-119del
IP: HA
HA-GPAT4
CHP1
cell lysate

Figure S5

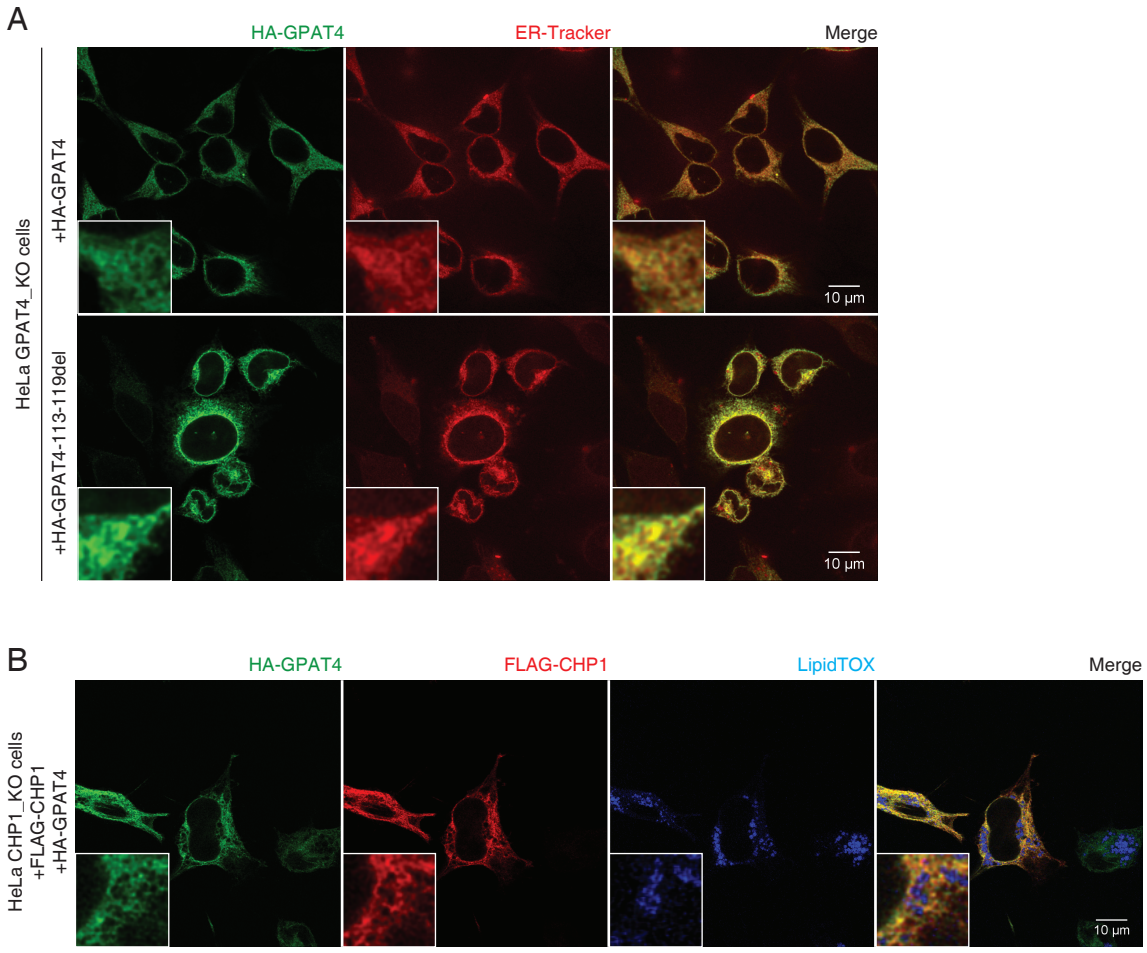
A
HA-GPAT4
ER-Tracker
Merge
HeLa GPAT4_KO cells
+HA-GPAT4
+HA-GPAT4-113-119del
10 μm
10 μm
B
HA-GPAT4
FLAG-CHP1
LipidTOX
Merge
HeLa CHP1_KO cells
+FLAG-CHP1
+HA-GPAT4
10 μm

Figure S6

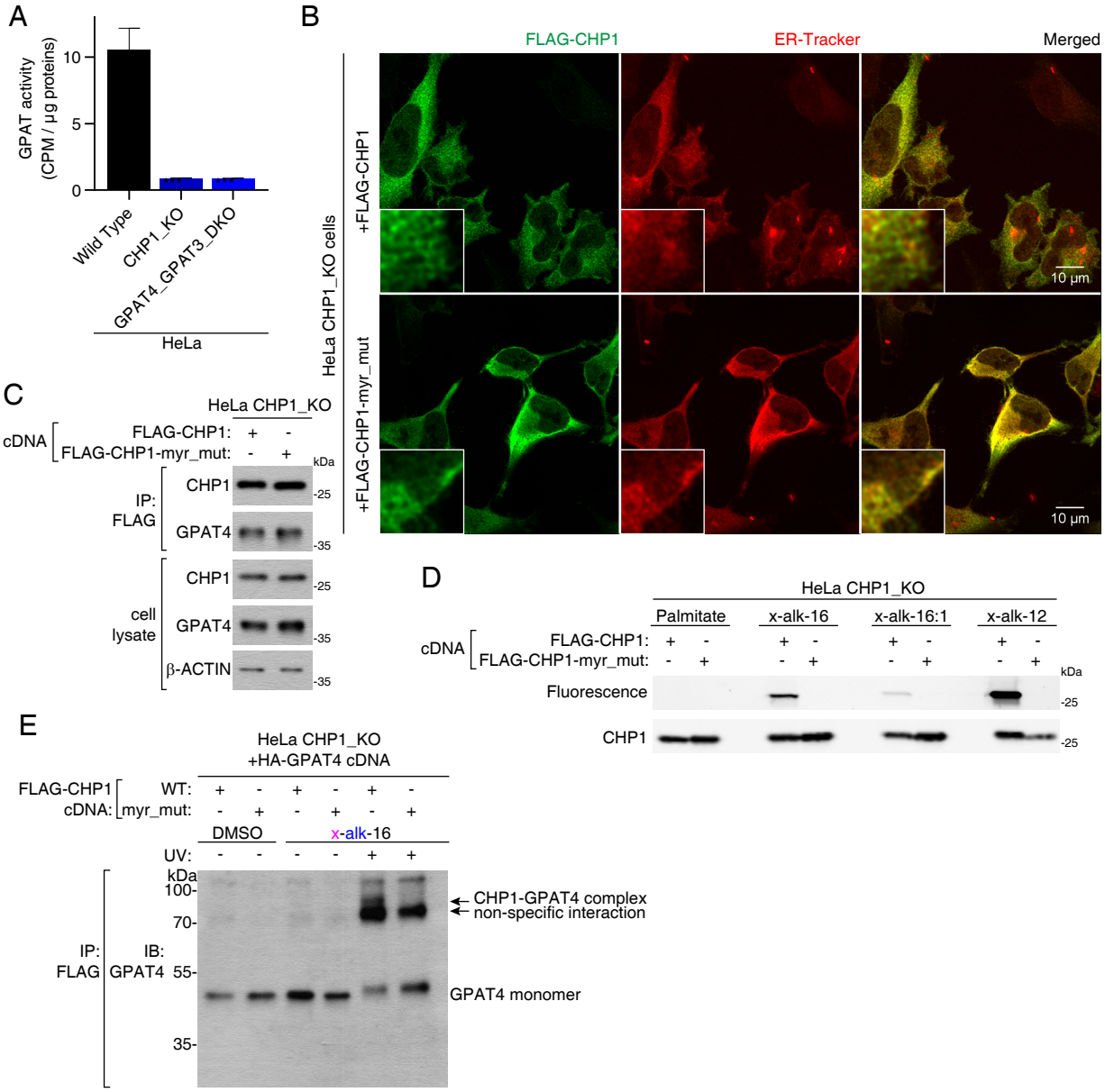
A
GPAT activity (CPM / µg proteins)
10
5
0
Wild Type
CHP1_KO
GPAT4_GPAT3_DKO
HeLa
B
FLAG-CHP1
ER-Tracker
Merged
HeLa CHP1_KO cells
+FLAG-CHP1
+FLAG-CHP1-myr_mut
10 µm
C
HeLa CHP1_KO
cDNA
FLAG-CHP1: + -
FLAG-CHP1-myr_mut: - +
kDa
IP: FLAG
CHP1
GPAT4
-25
-35
cell lysate
CHP1
GPAT4
β-ACTIN
-25
-35
-35
D
HeLa CHP1_KO
Palmitate
x-alk-16
x-alk-16:1
x-alk-12
cDNA
FLAG-CHP1: + - + - + - + -
FLAG-CHP1-myr_mut: - + - + - + - +
kDa
Fluorescence
CHP1
-25
-25
E
HeLa CHP1_KO
+HA-GPAT4 cDNA
FLAG-CHP1 cDNA: WT: + - + - + -
myr_mut: - + - + - +
DMSO
x-alk-16
UV: - - - - + +
kDa
100-
70-
55-
35-
IP: FLAG
IB: GPAT4
CHP1-GPAT4 complex
non-specific interaction
GPAT4 monomer

Figure S7

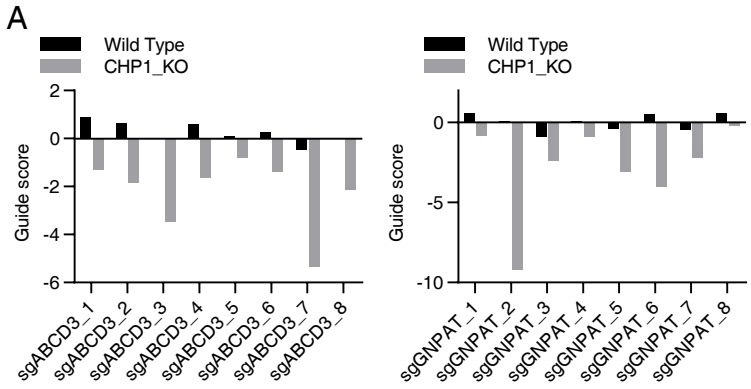
A
Wild Type
CHP1_KO
Guide score
2
0
-2
-4
-6
sgABCD3_1
sgABCD3_2
sgABCD3_3
sgABCD3_4
sgABCD3_5
sgABCD3_6
sgABCD3_7
sgABCD3_8
Wild Type
CHP1_KO
Guide score
0
-5
-10
sgGNPAT_1
sgGNPAT_2
sgGNPAT_3
sgGNPAT_4
sgGNPAT_5
sgGNPAT_6
sgGNPAT_7
sgGNPAT_8

Supplemental Figure Legends

Figure S1: ACSL4, ACSL3 and CHP1 are key regulators of adaptation to excess fatty acid, Related to Figure 1.

(A) Stimulated Raman scattering imaging of the indicated deuterium-labeled fatty acid treated HeLa cells. Intensity indicates the relative concentrations of labeled fatty acid metabolites. Scale bar, 20 μm.

(B) Immunoblot analysis of HeLa cells treated with 500 μM palmitate for the indicated durations. Cleaved PARP was used to show the extent of cell death. GAPDH was used as a loading control.

(C) Relative abundance of indicated lipid groups in Jurkat cells treated with 50 uM and 200 uM palmitate after a 24-hour treatment. Lipid species of the same group were summed. Values were normalized to the average of the untreated controls (n=3).

(D) Guide scores (log_2 fold change) of individual sgRNAs targeting ACSL4 used in the negative screen in the presence (gray) or absence (black) of palmitate.

(E) Differential guide scores ((palmitate)-(untreated)) of individual sgRNAs targeting ACSL3 and CHP1 used in the positive screen.

(F) Relative cell numbers of Jurkat wild type (black) and two clones of ACLS4_KO cells (blue) after a 4-day treatment with the indicated palmitate concentrations. Cell numbers were normalized to the untreated control (mean ± SD, n=3). *p < 0.05 versus wild type.

(G) Relative cell numbers of Jurkat wild type (black) and two clones of ACLS3_KO cells (blue) after a 4-day treatment with the indicated palmitate concentrations. Cell numbers were normalized to the untreated control (mean ± SD, n=3). **p < 0.01, ***p < 0.001 versus wild type.

(H) Relative cell numbers of Jurkat wild type (black) and two clones of CHP1_KO cells (blue) after a 4-day treatment with the indicated palmitate concentrations. Cell numbers were normalized to the untreated control (mean ± SD, n=3). **p < 0.01, ***p < 0.001 versus wild type.

(I) Fold change in cell number (log_2) of HepG2 wild type (black), ACSL4_KO (blue), ACSL3_KO and CHP1_KO (gray) cells after a 4-day treatment with the indicated palmitate concentrations (mean ± SD, n=3). *p < 0.05, **p < 0.01, ***p < 0.001 versus wild type.

Abbreviations for lipid groups used above and in subsequent figures: acylcarnitine (AcCa), ceramides (Cer), triacylglycerol (TG), lysophosphatidylethanolamine (LPE), phosphatidylinositol phosphate (PIP), diacylglycerol (DG), cardiolipin (CL), sphingomyelin(phytosphingosine) (phSM), phosphatidylglycerol (PG), phosphatidylinositol (PI), phosphatidic acid (PA), phosphatidylserine (PS), neutral glycosphingolipid (CerG1), phosphatidylethanolamine (PE), monoacylglycerol (MG), phosphatidylcholine (PC), lysophosphatidylcholine (LPC) and sphingomyelin (SM).

Figure S2: CHP1 loss prevents fatty acid incorporation and lipid accumulation, Related to Figure 2.

(A) Relative difference in abundance of triacylglycerol (TG) species ranked by saturation (number of double bonds) of the indicated cell lines. Values were normalized to the average of the wild type Jurkat cells (n=3).

(B) Fold change in cell number (log_2) of Jurkat cells after a 4-day treatment with the indicated fatty acid concentrations (mean ± SD, n=3). ***p < 0.001.

(C) Guide scores (log_2 fold change) of individual sgRNAs targeting ACSL3, ACSL4 and CHP1 used in the arachidonate screen in the presence (gray) or absence (black) of arachidonate.

(D) Normalized d-fatty acid abundance within wild type and CHP1_KO HeLa cells used in **Figure 2D** as indicated by C-D/CH_3 ratio. d-fatty acid intensity (C-D signal) was normalized to total protein intensity (CH_3 signal) to obtain normalized d-fatty acid level (mean ± SD, n=3). ***p < 0.001 versus wild type.
(E) Immunoblot analysis of wild type and CHP1_KO 3T3-F442A cells used in **Figure 2F**. β-actin was used as a loading control.
(F) Fold change (log_2) in the abundance of triacylglycerols of wild type and CHP1_KO 3T3-F442A preadipocytes. Values were normalized to the average of the wild type cells (mean ± SD, n=3). ***p < 0.001 versus wild type.
(G) Relative mRNA expression levels of indicated adipocyte differentiation markers in wild type and CHP1_KO 3T3-F442A cells collected on the indicated days upon start of differentiation. Minimal differences in differentiation were seen in the CHP1_KO cells. Expression levels were normalized to *Rpl32* (mean ± SD, n=3). **p < 0.01, ***p < 0.001 versus wild type.
(H) Phylogenetic comparison of CHP1 orthologues and paraglogues in metazoans. Protein sequences and comparisons were obtained from Ensembl (EMBL-EBI). CHP1 orthologues were highlighted in blue. Lowest peptide similarity in each group were shown.
(I) Fold change (log_2) in the abundance of triacylglycerols of wild type and *pbo-1*_KD *C. elegans*. Values were normalized to the average of the wild type animals (mean ± SD, n=3). *p < 0.05 versus wild type.
(J) Relative quantification of *elm* mRNA levels in the control and *elm*_KD flies. *Drosophila UAS-elm* RNAi or *UAS-White* RNAi transgenes were expressed under *Actin5C Gal4* driver. *White* RNAi served as control. Expression levels were normalized to *Rpl32* (mean ± SD, n=6). **p < 0.01 versus wild type.
(K) Fold change (log_2) in the abundance of triacylglycerols of control and *elm*_KD *D. melanogaster* midgut. Values were normalized to the average of the control animals (mean ± SD, n=3). ***p < 0.001 versus wild type.
(L) Fat bodies from 5-days old adult flies were fixed and stained with Nile red. Representative images of Nile red fluorescence (green) in the indicated animals were shown. Scale bar, 50 μm.

Figure S3: CHP1 ablation alters metabolite abundance in the glycerolipid synthesis pathway, Related to Figure 3.
(A) Fold change (log_2) in indicated lipid groups of Jurkat wild type, CHP1_KO and rescued CHP1_KO cells treated with 50μM palmitate for 24 hrs prior to lipid extraction. Lipid species of the same group were summed. Values were normalized to the average of the wild type untreated cells (mean ± SD, n=3). ***p < 0.001.
(B) Maximal exogenous fatty acid oxidation of wild type and CHP1_KO HeLa cells measured by Seahorse Fatty Acid Oxidation Assay (mean ± SD, n=3).
(C) Fold change (log_2) in the abundance of palmitoyl-CoA of wild type, ACSL3_KO and CHP1_KO Jurkat cells treated with 50μM palmitate for 24 hrs prior to metabolite extraction. Values were normalized to the average of the untreated wild type cells (mean ± SD, n=3). **p < 0.01, ***p < 0.001.
(D) Fold change (log_2) in the abundance of acylcarnitine of wild type and *pbo-1*_KD *C. elegans*. Values were normalized to the average of the wild type animals (mean ± SD, n=3). *p < 0.05 versus wild type.

(E) Fold change (log_2) in the abundance of acylcarnitine of control and *elm*_KD *D. melanogaster* midgut. Values were normalized to the average of the control animals (mean ± SD, n=3). **p < 0.01 versus control.

Figure S4: CHP1 interacts with GPAT4 and this interaction is required for GPAT4 function, Related to Figure 4.

(A) Motif analysis of CHP1 amino acid sequence. Analysis was carried out using MyHits (SIB).

(B) Immunoprecipitation of endogenous GPAT4 protein in HeLa cells. Anti-GPAT4 immunoprecipitates were prepared from cell lysates and analyzed by immunoblotting for levels of indicated proteins.

(C) CHP1 co-essentiality analysis using data from Wang et al. (2017). Gene correlation scores with CHP1 were calculated for all genes and ranked. The top co-essential gene is GPAT4 (red). Other GPATs (blue) do not correlate well with CHP1.

(D) Changes in lipid profiles of Jurkat wild type, CHP1_KO, GPAT4_KO and GPAT3_KO cells treated with control BSA or 50μM palmitate for 24 hrs prior to lipid extraction. Lipid species of the same group were summed. Values were normalized to the average of the untreated wild type controls (n=3).

(E) Fold change in cell number (log_2) of Jurkat wild type (black) and two clones of GPAT4_KO (blue) cells after a 4-day treatment with the indicated palmitate concentrations (mean ± SD, n=3). ***p < 0.001 versus wild type.

(F) Immunoblot analysis of HeLa wild type and CHP1_KO cells treated with 100μg/mL cycloheximide for the indicated durations. β-actin was used as a loading control (top). Densitometry analysis of GPAT4 protein levels from the above immunoblot. GPAT4 level was normalized to the initial (t=0) (bottom).

(G) Immunoblot analysis of HeLa wild type, GPAT4_KO, rescued GPAT4_KO, CHP1_KO and rescued CHP1_KO cells. β-actin was used as a loading control.

(H) Relative mRNA expression levels of *Chp1* and *Gpat4* in the indicated HeLa cell lines. Expression levels were normalized to *Rpl32* (mean ± SD, n=3).

(I) Identification of terminal regions of GPAT4 responsible for CHP1 interaction. Plasmids containing cDNA for HA-GPAT4 mutants with N- or C-terminal deletions, as well as full length HA-GPAT4, were expressed in HeLa rescued CHP1_KO cells. Immunoblot of co-immunoprecipitates with the indicated HA-GPAT4 constructs.

(J) Indicated deletions and full length HA-tagged GPAT4 cDNAs were expressed in HeLa cells.

(K) Interaction of CHP1 with large N-terminal deletions of HA-tagged GPAT4. Indicated deletions and full length HA-tagged GPAT4 cDNA were expressed in HeLa cells. Anti-HA immunoprecipitates were prepared from cell lysates and analyzed by immunoblotting for levels of indicated proteins.

(L) Interaction of CHP1 with full length and small 113-119del HA-tagged GPAT4 accounting for the reduction of CHP1 levels in GPAT4_KO cells. Indicated deletion and full length HA-tagged GPAT4 cDNA were expressed in HeLa cells. Anti-HA immunoprecipitates were prepared from cell lysates of cells expressing full length and 3X the amount of cells expressing 113-119del HA-GPAT4 and analyzed by immunoblotting for levels of indicated proteins.

Figure S5: GPAT4 interaction mutant does not affect localization of GPAT4, Related to Figure 4.

(A) Representative confocal immunofluorescence images of HeLa GPAT4_KO cells expressing wild type or interaction deficient (113-119del) HA-GPAT4. Stains for HA (green) and ER (red) were used. Insets show 5X magnified images. Scale bar, 10 μm.
(B) Representative confocal immunofluorescence images of HeLa CHP1_KO cells expressing FLAG-CHP1 and HA-GPAT4, treated with 1mM oleate. Stains for HA (green), FLAG (red) and neutral lipids (blue) were used. Insets show 5X magnified images. Scale bar, 10 μm.

Figure S6: CHP1 myristoylation mutant does not affect localization or GPAT4 interaction, Related to Figure 5.
(A) Radiolabeled GPAT activity assay of the indicated HeLa cell lines. Cell lysates were incubated with [^{14}C]-glycerol-3-phosphate. GPAT activity was quantified as the CPM in the non-polar fraction (mean ± SD, n=3). ***$p < 0.001$ versus wild type.
(B) Representative confocal immunofluorescence images of HeLa CHP1_KO cells expressing wild type or myristoylation mutant FLAG-CHP1. Stains for FLAG (green) and ER (red) were used. Insets show 5X magnified images. Scale bar, 10 μm.
(C) Immunoblot of co-immunoprecipitates with the indicated FLAG-CHP1 constructs. β-actin was used as a loading control.
(D) Immunoblot and in-gel fluorescence analysis of bifunctional fatty acid incorporation. HeLa CHP1_KO cells expressing the indicated FLAG-CHP1 constructs were incubated with 500 μM of the indicated bifunctional fatty acids or control palmitate for 24 hrs prior to immunoprecipitation. Fluorescence indicates incorporation of fatty acids through click chemistry with azido-rhodamine.
(E) Immunoblot using antibody against GPAT4 on immunoprecipitates with FLAG-CHP1 or FLAG-CHP1-myr_mut in the presence or absence of x-alk-16 photo-crosslinking. Crosslinked complex of CHP1-GPAT4 appeared as a higher band with a combined molecular weight of these two proteins (~80 kDa).

Figure S7: ABCD3 and GNPAT are required for cell survival upon loss of CHP1, Related to Figure 6.
(A) Guide scores (log_2 fold change) of individual sgRNAs targeting ABCD3 and GNPAT used in the isogenic screen in wild type (black) or CHP1_KO (gray) cells.